

# Role of Desolvation Energy in the Nonfacilitated Membrane Permeability of Dideoxyribose Analogs of Thymidine

LOIS L. WRIGHT and GEORGE R. PAINTER

Division of Virology, Burroughs Wellcome Co., Research Triangle Park, North Carolina 27709

Received October 14, 1991; Accepted January 27, 1992

## SUMMARY

The ability of thymidine and four dideoxyribose analogs of thymidine to cross phase barriers, such as those encountered at the *exo* and *endo* faces of a membrane, has been studied in a two-phase water/chloroform system. The rate constants for entering,  $k_a$ , and leaving,  $k_b$ , the organic phase and the partition coefficient,  $K_p$  ( $k_a/k_b$ ), were determined for each compound. The values of  $K_p$  were found to be proportional to the values of the rate constants for nonfacilitated diffusion,  $c$ , into human erythrocytes reported in the preceding paper [Mol. Pharmacol. 41:950-956 (1992)]. This linear relationship suggests that, in accord with the solubility-diffusion model of nonmediated membrane permeation, movement of the thymidine analogs across the potential energy barriers at the membrane interfaces is fast, relative to the rate of transbilayer diffusion. Because the com-

pounds have similar molecular volumes and would, therefore, have similar rates of transbilayer diffusion, the differences in  $c$  reflect the differences in the distribution of the compounds across the interfaces, i.e., the  $K_p$  values. The magnitudes of the  $K_p$  values are dependent not only on the  $\pi$  value of each substituent on the dideoxyribose ring but also on the position of the substituent. Analogs having a hydroxyl group in the 5'-position have a higher  $K_p$  and a higher  $c$  than the corresponding analogs with the hydroxyl group in the 3'-position. This increased lipophilicity is attributed to a decrease in desolvation energy, resulting from the ability of the 5'-hydroxyl analogs to assume a *syn* configuration in which a bifurcated, intramolecular, hydrogen bond can be formed to the O-4' and the C-2 carbonyl groups.

Many classes of small organic molecules (1), including certain nucleosides and nucleoside analogs (2-8), can effectively permeate biomembranes by nonfacilitated diffusion. The mechanism of passive diffusion has been studied extensively (9-11). One model of passive membrane permeation has been proposed using transition state theory. In this model, the phospholipid matrix of the membrane is visualized as a potential energy barrier (Fig. 1) (11-13). The barrier may be separated into a number of discrete potential energy jumps. The initial jump,  $\mu_a$ , is crossed when moving from the extracellular aqueous phase into the apolar membrane interior. Any number of successive jumps of height  $\mu_e$  are encountered within the interior of the phospholipid bilayer. The final jump,  $\mu_b$ , is encountered when leaving the membrane and moving into the intracellular aqueous phase. The magnitude of  $\mu_a$  and  $\mu_b$  and, consequently, the respective rates,  $k_a$  and  $k_b$ , at which a molecule is able to cross the potential energy barriers at the *exo* and *endo* faces of the membrane are to a large extent determined by desolvation energy (12, 14). This energy is, in turn, dependent on the number of hydrogen-bond donors and acceptors that a solute contains (14) and the availability of these moieties to interact with solvent (15-17).

We describe the use of a stacked, two-phase, water/chloroform system to study the molecular properties that modulate the ability of dThd and four dideoxyribose analogs of dThd (Fig. 2) to partition across a phase barrier such as that encountered at a membrane interface. The partition coefficient for distribution of a nonelectrolyte from the aqueous phase into a membrane bilayer has been shown to be related to the partition coefficient for distribution into a nonpolar organic solvent (14, 18). Chloroform, which has been used extensively as a model of the apolar interior of biological membranes (14, 19-21), was used in the present study as the organic lipophilic phase. Movement of an organic molecule from an aqueous environment to chloroform requires complete desolvation. This is in contrast to protic organic solvents, such as the more commonly used *n*-octanol, which solubilize partially hydrated organic molecules and are, consequently, less sensitive to small changes in desolvation energy (22). The rate constants for transfer from water to chloroform,  $k_a$ , and from chloroform to water,  $k_b$ , and the partition coefficient,  $K_p$ , were determined for each compound by monitoring the disappearance of the compound from the aqueous phase. Comparison of these results with the  $c$  values reported in the preceding paper (23) indicates that, in

**ABBREVIATIONS:** dThd, thymidine; 3'-ddThd, 3'-deoxythymidine; 3'-N<sub>3</sub>-3'-ddThd, 3'-azido-3'-deoxythymidine; 5'-ddThd, 5'-deoxythymidine; 5'-N<sub>3</sub>-5'-ddThd, 5'-azido-5'-deoxythymidine; HEPES, 4-(2-hydroxyethyl)-1-piperazineethanesulfonic acid; *o*-OH-BA, *o*-hydroxybenzoic acid; *p*-OH-BA, *p*-hydroxybenzoic acid.

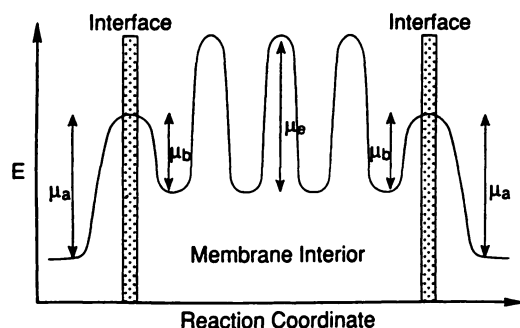
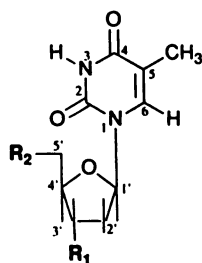


**Fig. 1.** Potential energy diagram of the aqueous interfaces of the phospholipid bilayer. The energy barriers,  $\mu_a$  and  $\mu_b$ , are met upon entering and leaving, respectively, the apolar membrane interior. Because diffusion through the bilayer is non-Stokesian (31), the solute does not encounter a resistance continuum but, instead, encounters an intermittent resistance, which can be represented by a series of barriers of height  $\mu_a$ . The relative heights of  $\mu_a$ ,  $\mu_b$ , and  $\mu_a$  depend upon the physicochemical properties of the solute and the composition of the bilayer. In the case depicted here, the rate-limiting step for transfer across the entire membrane is diffusion through the membrane interior. A more generalized model of the permeation barriers that allows for membrane inhomogeneity and local partition coefficients has been discussed by Diamond and Katz (18).



Compound	R <sub>1</sub>	R <sub>2</sub>
dThd	OH	OH
3'-ddThd	H	OH
5'-ddThd	OH	H
3'-N <sub>3</sub> -3'-ddThd	N <sub>3</sub>	OH
5'-N <sub>3</sub> -5'-ddThd	OH	N <sub>3</sub>

**Fig. 2.** Chemical structures of dThd and four dideoxyribose analogs.

accord with the solubility-diffusion model of membrane permeability (24, 25),  $c$  is directly proportional to  $K_p$ . The magnitudes of the  $K_p$  values are dependent not only on the lipophilicity of the substituents on the dideoxyribose ring but also on the position of the substituents. Analogs with the hydroxyl group in the 5'-position are more lipophilic than their counterparts with the hydroxyl group in the 3'-position. This difference is attributed to the ability of analogs with the hydroxyl group in the 5'-position to form bifurcated, intramolecular, hydrogen bonds to O-4' and the C-2 carbonyl group. Formation of this hydrogen bond decreases the energy required to desolvate the molecule, as evidenced by a faster transfer rate out of the aqueous phase,  $k_a$ , and increases stability in apolar media, as evidenced by a slower transfer rate out of the organic phase,  $k_b$ .

## Experimental Procedures

**Materials.** dThd was purchased from United States Biochemical Corp. (Cleveland, OH). 3'-ddThd, 3'-N<sub>3</sub>-3'-ddThd, 5'-ddThd, and 5'-N<sub>3</sub>-5'-ddThd were synthesized in these laboratories, according to pub-

lished procedures (26–28). The purity of these compounds was determined by <sup>1</sup>H and <sup>13</sup>C NMR. Salicylic acid (*o*-OH BA) and *p*-OH BA were obtained from Sigma (St. Louis, MO) and used without further purification. Spectrophotometric grade chloroform was from Aldrich (Milwaukee, WI), HEPES buffer was from Flow Laboratories (McLean, VA), and 0.9% sodium chloride was from Baxter Healthcare Corp. (Deerfield, IL).

**Experimental apparatus.** The stacked two-phase system is a modification of that previously reported by Pressman (19). Ten milliliters of 10 mM HEPES-saline (pH 7.3), containing the compound to be tested, were carefully layered onto 10 ml of chloroform (stabilized with 5.5–6.0%, v/v, ethanol), in a cylinder (outer diameter, 2.2 cm) (Fig. 3). The same cylinder was used for all experiments. The temperature was maintained at 37° by immersion in a constant-temperature water bath. The organic layer was stirred from below, with a magnetic stirring bar driven by a Spincadet immersible electromagnetic stirrer (Cole-Parmer, Chicago, IL). The stirring bar rotated at a maximum of 240 rpm and alternated direction every 2 sec. Periodically reversing the rotation of the stirring bar prevented vortexing and disruption of the phase barrier. By using sufficiently high concentrations of solute and vigorous stirring of the organic phase, the effects of unstirred layers on observed transfer rates can often be eliminated (29). The applicability of this statement to the stacked two-phase system was confirmed by varying the stirring speed between 75 and 500 rpm and monitoring the effects on  $k_a$  and  $k_b$ . The resultant values for  $k_a$  and  $k_b$  for each of the compounds were invariant above 100 rpm, confirming that, with adequate stirring of the organic phase, unstirred-layer effects do not influence observed transfer rates in this system.

**Transfer rates.** The rate of transfer of the compound across the water/chloroform phase barrier was monitored by measuring the absorbance of 10- $\mu$ l aliquots withdrawn from the aqueous phase, with a Hamilton syringe, at regular intervals (the stirrer was turned on at  $t = 0$ ). Each 10- $\mu$ l aliquot was added to a cuvette containing 1 ml of buffered saline, and the absorbance was measured at 267 nm, the  $\lambda_{max}$  for each of the compounds, using a Perkin-Elmer Lambda 6 spectrophotometer. Each experiment was continued until the system had reached equilibrium. 3'-N<sub>3</sub>-3'-ddThd, 5'-N<sub>3</sub>-5'-ddThd, 3'-ddThd, 5'-ddThd, and dThd obeyed Beer's law at 267 nm over the concentration range used in the study (2 mM to 10 mM).

**Kinetic analysis.** Assuming a first-order reversible reaction at the phase barrier (30), the rate equation describing movement of a compound across the barrier is

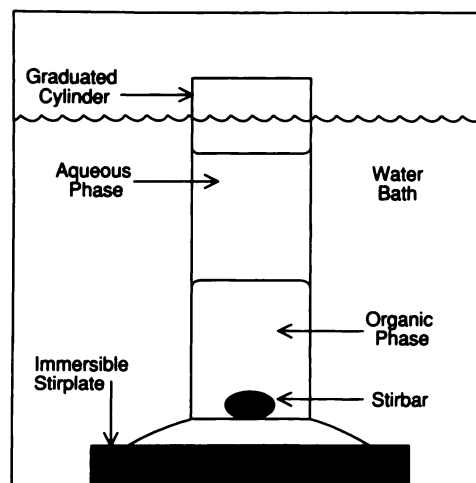


**Fig. 3.** Apparatus used in the stacked, two-phase, rate of transfer experiments. The organic phase was spectrophotometric grade chloroform stabilized with 5.5–6.0% (v/v) ethanol. The aqueous phase was 10 mM HEPES-saline (0.9%) buffer (pH 7.3). The temperature was maintained at 37° by immersion in a constant-temperature water bath.

$$\frac{-dS}{dt} = k_a S - k_b (S_o - S) \quad (1)$$

where  $S$  is the concentration of compound in the aqueous phase at any time  $t$ ,  $S_o$  is the concentration in the aqueous phase at time  $t = 0$ ,  $k_a$  is the rate constant for movement into the organic phase, and  $k_b$  is the rate constant for movement out of the organic phase. Solving this differential equation yields

$$S(t) = S_o / (k_a + k_b) \cdot \{k_b + k_a \cdot \exp(-(k_a + k_b)t)\} \quad (2)$$

At  $t = \infty$ , thermochemical equilibrium has been achieved, and eq. 2 simplifies to

$$S_\infty = S_o \cdot k_b / (k_a + k_b) \quad (3)$$

Each data set was fit to eq. 2, using nonlinear least-squares regression analysis, to determine  $k_a$  and  $k_b$ .

**Partition coefficients.** The ratio of the concentration of the compound in each phase,  $K_p$ , was determined by two different techniques.  $K_p^f$  was calculated from the equation

$$K_p^f = (S_o - S_\infty) / S_\infty = k_a / k_b \quad (4)$$

where  $S_\infty$  is determined from the fit of the transfer rate data to eqs. 2 and 3. Alternatively, chloroform and buffer containing compound of initial concentration  $S_i$  were warmed to 37°, added in equal volumes to a Pyrex screw-top test tube, and vortexed for 5 min on a Fisherbrand Vortex Genie 2. Vortexing for longer times did not affect the results. The aqueous and organic phases were allowed to separate (<1 min), and an aliquot of the aqueous phase was centrifuged (Fisher model 235C) at 13,600 ×  $g$  for 5 min, to spin down any chloroform emulsions. The absorbance of a 10- $\mu$ l aliquot from the centrifuged sample was measured as described above, to determine the final concentration of compound in the aqueous layer,  $S_f$ .  $K_p^v$  was then calculated from the equation

$$K_p^v = (S_i - S_f) / S_f \quad (5)$$

## Results

A typical time course for equilibration across the water/chloroform phase barrier is shown for the case of 3'-N<sub>3</sub>-3'-ddThd in Fig. 4. Values of  $k_a$  and  $k_b$  were generated for each of the five compounds from a fit of eq. 2 to the time course data, as described in Experimental Procedures. For each experiment, the error in the fit of the equation to the data was <10%. Compliance of each of the equilibration reactions with the

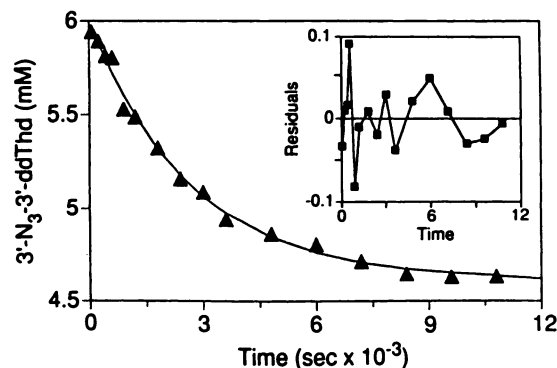


**Fig. 4.** Plot of the decrease in the concentration of 3'-N<sub>3</sub>-3'-ddThd in the aqueous phase as a function of time. The solid line is the result of nonlinear least-squares regression analysis of the data according to eq. 2. *Inset*, plot of the residuals, which indicates that the data fit well to the model described by eq. 2. These results are representative of all the rate of transfer experiments.

interfacial transfer model described by eq. 2 indicates that the transfer reactions are first order with respect to the concentration of permeant. The results are summarized in Table 1. Each rate constant is the average of four separate determinations carried out at values of  $S_o$  between 2 and 10 mM. Because of the minimal solubility of dThd in organic solvents and limitations on the sensitivity of this technique imposed by the signal to noise ratio of the spectrophotometer, the rate of transfer of dThd across the phase barrier could not be determined accurately at initial concentrations lower than 6 mM. Therefore, all experiments in which dThd was the permeant used initial concentrations between 6 and 10 mM.

$K_p^f$  values calculated from the rate data in Table 1, using eq. 4, and  $K_p^v$  values determined from vortex experiments are shown in Table 2. The vortexing experiments were carried out to establish an end-point for distribution across the phase barrier and to ensure that the duration of the transfer experiments was sufficient to allow the system to achieve thermochemical equilibrium. The  $K_p^f$  values for 5'-N<sub>3</sub>-5'-ddThd, 3'-ddThd, 5'-ddThd, and dThd are statistically indistinguishable from the  $K_p^v$  values. However, the  $K_p^f$  value for 3'-N<sub>3</sub>-3'-ddThd is somewhat higher than the corresponding  $K_p^v$  value. Extending the time course of the transfer experiment up to 6 hr did not result in an increase in  $K_p^f$  up to the level seen in the vortexing experiment. One explanation for the difference is that the thermal coefficient for transfer of the highly lipophilic 3'-N<sub>3</sub>-3'-ddThd is large, so that a small change in temperature, such as that caused by the conversion of mechanical energy from vortexing into heat (32), results in a change in  $K_p$ .

The relationship between the rate constant for the permeability of a biomembrane,  $c$ , and the partition coefficient,  $K_p$ , derived from the homogeneous, symmetric, membrane bilayer model shown in Fig. 1 is

$$c = k_a k_e / (k_b + 2k_e) \quad (6)$$

where  $k_e$  is the rate constant determined by the magnitude of the energy barrier(s),  $\mu_e$  (12, 13). Because the physical forces that modulate each of these rates are similar, it has often proven to be difficult to determine experimentally the rate-limiting step in the passive membrane-permeation process. In the solubility-diffusion model of membrane permeability, movement across the membrane interface is assumed to be fast, compared with the rate of diffusion across the bilayer interior (24, 25), i.e.,  $k_a$  and  $k_b \gg k_e$ , in which case eq. 6 simplifies to

$$c = k_a k_e / k_b = k_e K_p \quad (7)$$

A plot of eq. 7 made from the data in Table 2 is shown in Fig. 5. Values of  $c$  measured for these five nucleosides in erythro-

TABLE 1

**Rate constants for the transfer of dThd and four dideoxyribose analogs of dThd across a phase barrier**

The rate constants for crossing into ( $k_a$ ) and out of ( $k_b$ ) the chloroform phase were determined as described in Experimental Procedures. Each rate constant is the average of four separate determinations.

Compound	$k_a$	$k_b$
	$\text{sec}^{-1} \times 10^6$	$\text{sec}^{-1} \times 10^6$
3'-N <sub>3</sub> -3'-ddThd	$8.17 \pm 0.33$	$28.17 \pm 1.33$
5'-N <sub>3</sub> -5'-ddThd	$6.17 \pm 0.50$	$35.67 \pm 2.33$
3'-ddThd	$4.83 \pm 0.33$	$43.17 \pm 5.33$
5'-ddThd	$4.33 \pm 1.50$	$51.50 \pm 14.67$
dThd	$2.33 \pm 0.67$	$62.50 \pm 9.83$



TABLE 2

## Partition coefficients, rate constants, and molecular volumes for dThd and four dideoxyribose analogs of dThd

The partition coefficient for each compound was determined by two different techniques,  $K_p^f$  by fitting and  $K_p^v$  by vortexing, as described in Experimental Procedures. Each value of  $K_p^f$  and  $K_p^v$  is the average of six and three independent determinations, respectively. The rate constants for nonfacilitated diffusion into human erythrocytes,  $c$ , were reported by Zimmerman *et al.* (2) and Domin *et al.* (3, 23). The molecular volumes,  $V$ , were determined from models generated using MacroModel version 2.5 (31).

Compound	$K_p^f$	$K_p^v$	$c$ fmol/sec/ $\mu$ M/ 5 $\mu$ l of cells	$V$ $\text{\AA}^3$
3'-N <sub>3</sub> -3'-ddThd	0.293 $\pm$ 0.015	0.348 $\pm$ 0.009	110 $\pm$ 11	201.4
5'-N <sub>3</sub> -5'-ddThd	0.172 $\pm$ 0.006	0.181 $\pm$ 0.022	36 $\pm$ 3	208.6
3'-ddThd	0.119 $\pm$ 0.011	0.133 $\pm$ 0.005	30 $\pm$ 1	189.6
5'-ddThd	0.086 $\pm$ 0.010	0.102 $\pm$ 0.006	19 $\pm$ 2	194.8
dThd	0.036 $\pm$ 0.006	0.061 $\pm$ 0.008	<0.2	210.3
<i>o</i> -OH BA*	1.438 $\pm$ 0.080	1.447 $\pm$ 0.033		
<i>p</i> -OH BA*	0.058 $\pm$ 0.010	0.040 $\pm$ 0.008		

\* The *o*-OH- and *p*-OH-BA experiments were included as controls, to demonstrate that the kinetic and thermodynamic effects of intramolecular hydrogen bonding seen in the permeability of black lipid membranes are also observed in the stacked, two-phase system.

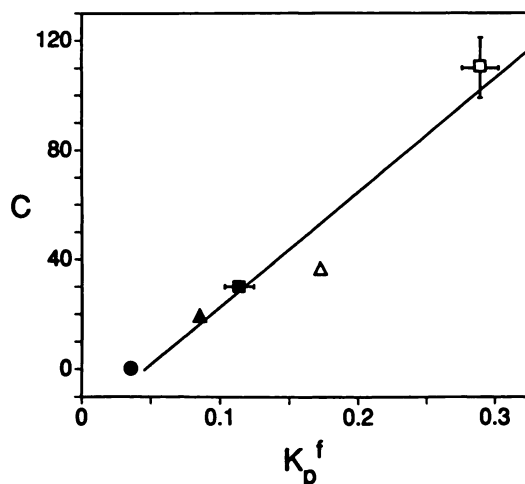


Fig. 5. Plot of  $c$  versus  $K_p^f$  for dThd and the four dideoxyribose analogs. ●, dThd; ▲, 5'-ddThd; ■, 3'-ddThd; △, 5'-N<sub>3</sub>-5'-ddThd; □, 3'-N<sub>3</sub>-3'-ddThd. The solid line is the result of linear least-squares regression analysis of the data ( $c = 420 \cdot K_p^f - 20$ ). Error bars did not extend beyond the data symbols for dThd, 5'-ddThd, and 5'-N<sub>3</sub>-5'-ddThd.

cytes (2, 3, 23) correlate, in a linear fashion ( $r^2 = 0.98$ ), with the values of  $K_p^f$  given in Table 2. Within the context of the solubility-diffusion model of nonfacilitated permeation, these results suggest transbilayer diffusion to be the rate-limiting step. Because the molecular volumes of the compounds differ by <10% (Table 2), values of  $k_s$  would be anticipated to be similar (33). Thus, the rate-determining step would be the same for each analog in the series, and differences in  $c$  would be dependent upon differences in  $K_p$ .

### Discussion

The correlation of  $K_p$  with  $c$  suggests that the molecular forces affecting the relative rate of permeation of erythrocyte membranes by the dideoxyribose analogs of dThd are very similar to those that determine the partition patterns of these compounds into chloroform. The ability of chloroform to discriminate between the compounds in this series, whereas *n*-octanol cannot (23), may be due to the higher selectivity factor,  $s$ , (18) for chloroform. It has been suggested, based on an analysis of incremental free energies of solution of specific functional groups in water, bulk lipids, and membranes, that the main pattern of selectivity is due largely to differences in

water/solute intermolecular forces (14, 18, 34). Examination of the interfacial rate constants in Table 1 shows that  $k_a$  ranges from being approximately 3- to 30-fold slower than the corresponding  $k_b$ . Indeed, the energy required to remove the compound from the aqueous medium determines the position of the partition equilibrium of each compound examined here. However, when comparisons are made between rate constants of compounds in the series, the most striking observation is that a decrease in  $k_a$  produced by an alteration of the dideoxyribose ring is accompanied by a proportional increase in  $k_b$ . As the molecules in the series become more polar (as indicated by a decrease in  $K_p$ ), not only do they move into the chloroform phase more slowly, but they also have a lower energy barrier for movement out of the chloroform phase. Thus, relative decreases in  $K_p$  within the series of compounds can be attributed to a decrease in the stability of the compound in the bulk lipid phase, as well as to increased desolvation energy. This observation is not surprising, because factors that stabilize a molecule in aqueous media tend to cause destabilization in apolar media (22).

The  $K_p$  values of dThd and the four dideoxyribose analogs increase in the order dThd < 5'-ddThd < 3'-ddThd < 5'-N<sub>3</sub>-5'-ddThd < 3'-N<sub>3</sub>-3'-ddThd. The overall order reflects the  $\pi$  value of the dideoxyribose substituent. Using the additivity of substituent constants,  $\pi$  values, to estimate relative lipophilicities (35, 36), substitution of an azido group for the 3'-hydroxyl group would be anticipated to produce an approximate 5-fold increase in  $K_p$  (observed = 8-fold), and substitution of a hydrogen for the 3'-hydroxyl would be anticipated to produce an approximate 3-fold increase in  $K_p$  (observed = 3-fold). The position of the substitution also determines the relative lipophilicity of the analogs. Analogs with the hydroxyl group in the 5'-position are more lipophilic than their counterparts with the hydroxyl group in the 3'-position. The positional effect is eliminated by acylation of the 3'- and 5'-hydroxyl groups, as shown for the case of 3'-ddThd and 5'-ddThd, where acylation results in the  $K_p$  values of both compounds increasing to  $1.72 \pm 0.36$ . The positional effect is quite large for the azido analogs, for which switching of the azido group from the 3'- to the 5'-position results in a 40% decrease in  $K_p$ . At present we have no explanation for the extremely large difference (40%) seen in the  $K_p$  values of 3'-N<sub>3</sub>-3'-ddThd and 5'-N<sub>3</sub>-5'-ddThd, relative to the difference in the  $K_p$  values measured for 3'-ddThd and 5'-ddThd (28%). We are presently investigating positional

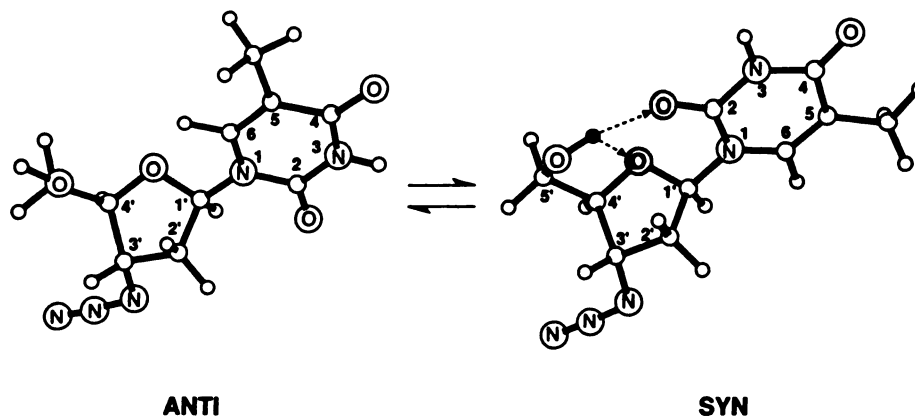


**Fig. 6.** *Syn-anti* equilibrium observed for 3'-N<sub>3</sub>-3'-ddThd in solution. The conformation of the *syn* form (right) places the 5'-hydroxyl group in a position to form a bifurcated hydrogen bond (dashed lines) to the O-4' moiety on the dideoxyribose ring and the C-2 carbonyl on the thymine ring. In the depiction of the *anti* form (left), the C-5' is eclipsed by O-5'.

isomers in another nucleoside series, seeking the source of this large effect.

Dideoxyribose analogs of dThd with the single hydroxyl group on the dideoxyribose ring in the 5'-position can form strong intramolecular hydrogen bonds (37). NMR studies carried out on 3'-N<sub>3</sub>-3'-ddThd in D<sub>2</sub>O and CDCl<sub>3</sub> have demonstrated that the switch from polar to apolar media is accompanied by a shift in the conformational equilibrium (Fig. 6) (37). In D<sub>2</sub>O, the thymine ring is predominantly in an *anti* orientation (92%, based on nuclear Overhauser effect measurements), and the 3'-azido-2',3'-dideoxyribose ring is in rapid exchange between an N (C-3' *endo*) and an S (C-2' *endo*) form. In CDCl<sub>3</sub>, nuclear Overhauser effect measurements indicate that the conformational equilibrium has shifted, with 42% of the population now in the *syn* configuration (Fig. 6). The 3'-azido-2',3'-dideoxyribose ring is still in rapid exchange between the N and S form. However, ring puckering has decreased from the value of 28° observed in D<sub>2</sub>O to 20°, due to the formation of a bifurcated hydrogen bond in which the 5'-hydroxyl is the donor and the O-4' and the C-2 carbonyl groups are acceptors. The shift toward the *syn* form in the apolar media is attributed to the stabilization of the 5'-hydroxyl provided by this intramolecular hydrogen bond.

The existence of the *anti-syn* equilibrium suggests that conformation is a factor in nucleosides crossing the interfacial barrier, whereby assumption of the *syn* configuration and formation of a strong intramolecular hydrogen bond reduces the magnitude of  $\mu_a$  by reducing the aqueous solvation energy and increases  $\mu_b$  by stabilizing the compound in apolar media. The 5'-hydroxyl group of 3'-ddThd is available for the formation of an intramolecular hydrogen bond analogous to that shown for 3'-N<sub>3</sub>-3'-ddThd in Fig. 6. However, there is no way to stabilize the 3'-hydroxyl on the dideoxyribose rings of 5'-N<sub>3</sub>-5'-ddThd or 5'-ddThd. In each case,  $k_a$  is less and  $k_b$  more than that of the corresponding analog with the hydroxyl group in the 5'-position (Table 1). Another example of the profound influence an intramolecular hydrogen bond can have on membrane permeability is provided by *o*-OH BA, which has a strong, permanent, intramolecular hydrogen bond. The permeation coefficient of this acid determined in black lipid membranes is 30-fold larger than that of *p*-OH BA (see Table 2 for control experiments in the two-phase system) (25, 38).

In summary, the correlation of  $K_p$  with  $c$  suggests that

equilibration of the dThd analogs across the membrane interface is fast, relative to the rate of diffusion across the apolar interior of the erythrocyte phospholipid bilayer. The  $K_p$  values of these compounds are dependent on both of the desolvation potential energy barriers,  $\mu_a$  and  $\mu_b$ . The magnitudes of  $\mu_a$  and  $\mu_b$  are not only a function of the lipophilicity of substituents on the dideoxyribose ring but are also dependent on the position of the substituent. Calculation of solvation energies using the solvent-accessible surface approach has shown that the *syn* form of 3'-N<sub>3</sub>-3'-ddThd has approximately 0.38 kcal/mol less interaction energy with water than 5'-N<sub>3</sub>-5'-ddThd (37). This difference in solvation energy can readily account for the 25% decrease seen in  $k_a$  upon moving the azido moiety from the 3'- to the 5'-position; because factors that destabilize in aqueous environments tend to stabilize in apolar environments, formation of the hydrogen bond can also account for the almost identical increase seen in  $k_b$ . These results emphasize the importance that conformational factors can have in determining solvation energies and, consequently, the rates of nonfacilitated membrane permeation of nonelectrolytes.

#### Acknowledgments

We would like to thank Dr. Janet Rideout, Dr. Susan Daluge, and Mr. Andy Freeman of the Division of Organic Chemistry, Burroughs Wellcome Co., for the dideoxyribose analogs of dThd.

#### References

- Goldstein, A., L. Aronow, and S. M. Kalman. *Principles of Drug Action*, Ed. 2. Wiley, New York (1974).
- Zimmerman, T. P., W. B. Mahony, and K. L. Prus. 3'-Azido-3'-deoxythymidine: an unusual nucleoside analogue that permeates the membrane of human erythrocytes and lymphocytes by nonfacilitated diffusion. *J. Biol. Chem.* **262**:5748-5754 (1987).
- Domin, B. A., W. B. Mahony, and T. P. Zimmerman. 2',3'-Dideoxythymidine permeation of the human erythrocyte membrane by nonfacilitated diffusion. *Biochem. Biophys. Res. Commun.* **154**:825-831 (1988).
- Ahluwalia, G., D. A. Cooney, H. Mitsuya, A. Fridland, K. P. Flora, Z. Hao, S. Dalal, S. Broder, and D. G. Johns. Initial studies on the cellular pharmacology of 2',3'-dideoxyinosine, an inhibitor of HIV infectivity. *Biochem. Pharmacol.* **36**:3797-3800 (1987).
- Plagemann, P. G. W., and C. Woffendin. Permeation and salvage of dideoxyadenosine in mammalian cells. *Mol. Pharmacol.* **36**:185-192 (1989).
- Masood, R., G. S. Ahluwalia, D. A. Cooney, A. Fridland, V. E. Marquez, J. S. Driscoll, Z. Hao, H. Mitsuya, C. F. Perno, S. Broder, and D. G. Johns. 2'-Fluoro-2',3'-dideoxyarabinothymine: a metabolically stable analogue of the antiretroviral agent 2',3'-dideoxyadenosine. *Mol. Pharmacol.* **37**:590-596 (1990).
- Busso, M. E., L. Resnick, B. H. Yang, and A. M. Mian. Cellular pharmacology and anti-HIV activity of 2',3'-dideoxyguanosine. *AIDS Res. Hum. Retroviruses* **6**:1139-1146 (1990).
- August, E. M., E. M. Birks, and W. H. Prusoff. 3'-Deoxythymidin-2'-ene

- permeation of human lymphocyte H9 cells by nonfacilitated diffusion. *Mol. Pharmacol.* **39**:246-249 (1991).
9. Miller, D. M. Evidence that interfacial transport is rate-limiting during passive cell membrane permeation. *Biochim. Biophys. Acta* **1065**:75-81 (1991).
  10. Miller, D. M. The measurement of the rate of transport of solutes in both directions across the aqueous-nonaqueous liquid interface and its significance to membrane permeability. *Biochim. Biophys. Acta* **856**:27-35 (1986).
  11. Stein, W. D. *Transport and Diffusion across Cell Membranes*. Academic Press, New York (1986).
  12. Davson, H., and J. F. Danielli. *The Permeability of Natural Membranes*. Cambridge University Press, Cambridge, UK (1943).
  13. Zwolinski, B. J., H. Eyring, and C. E. Reese. Diffusion and membrane permeability. *J. Phys. Colloid Chem.* **53**:1426-1453 (1949).
  14. Stein, W. D. *The Movement of Molecules Across Cell Membranes*. Academic Press, New York (1967).
  15. Painter, G. R., R. Pollack, and B. C. Pressman. Conformational dynamics of the carboxylic ionophore Laasalocid A underlying cation complexation-decomplexation and membrane transport. *Biochemistry* **21**:5613-5620 (1982).
  16. Painter, G. R., and B. C. Pressman. Dynamic aspects of ionophore mediated membrane transport. *Top. Curr. Chem.* **101**:83-110 (1982).
  17. Caughey, B., G. R. Painter, A. F. Drake, and W. A. Gibbons. The role of molecular conformation in ion capture by carboxylic ionophores: a circular dichroism study of narasin A in single-phase solvents and liposomes. *Biochim. Biophys. Acta* **854**:109-116 (1986).
  18. Diamond, J. M., and Y. Katz. Interpretation of nonelectrolyte partition coefficients between dimyristoyl lecithin and water. *J. Membr. Biol.* **17**:121-154 (1974).
  19. Pressman, B. C. Mechanism of action of transport-mediating antibiotics. *Anal. N. Y. Acad. Sci.* **147**:829-841 (1969).
  20. Benzing, T., T. Tjivikua, J. Wolfe, and J. Rebek, Jr. Recognition and transport of adenine derivatives with synthetic receptors. *Science (Washington D. C.)* **242**:266-268 (1988).
  21. Rebek, J., Jr., B. Askew, D. Nemeth, and K. Parris. Convergent functional groups. 4. Recognition and transport of amino acids across a liquid membrane. *J. Am. Chem. Soc.* **109**:2432-2434 (1987).
  22. Reichardt, C. *Solvents and Solvent Effects in Organic Chemistry*. VCH Publishers, New York (1988).
  23. Domin, B. A., W. B. Mahony, G. W. Koszalka, D. J. T. Porter, G. Hajian, and T. P. Zimmerman. Membrane permeation characteristics of 5'-modified thymidine analogs. *Mol. Pharmacol.* **41**:950-956 (1992).
  24. Finkelstein, A. Water and nonelectrolyte permeability of lipid bilayer membranes. *J. Gen. Physiol.* **68**:127-135 (1976).
  25. Wolosin, J. M., and H. Ginsburg. The permeation of organic acids through lecithin bilayers: resemblance to diffusion in polymers. *Biochim. Biophys. Acta* **389**:20-33 (1975).
  26. Sekine, M., and T. Nakanishi. Facile synthesis of 3'-O-methylthymidine and 3'-deoxythymidine and related deoxygenated thymidine derivatives: a new method for selective deoxygenation of secondary hydroxy groups. *J. Org. Chem.* **55**:924-928 (1990).
  27. Horwitz, J. P., J. Chua, and M. Noel. Nucleosides. V. The monomesylates of 1-(2'-deoxy- $\beta$ -D-lyxofuranosyl)thymine. *J. Org. Chem.* **29**:2076-2078 (1964).
  28. Yamamoto, I., M. Sekine, and T. Hata. One-step synthesis of 5'-azido-nucleosides. *J. Chem. Soc. Perkin Trans. I* **1**:306-310 (1980).
  29. Sollner, K. The basic electrochemistry of liquid membranes, in *Diffusion Processes, Proceedings of the Thomas Graham Memorial Symposium, University of Strathclyde* (J. N. Sherwood, A. V. Chadwick, W. M. Muir, and F. L. Swinton, eds.). Gordon and Breach, London, 655-730 (1971).
  30. Skinner, G. B. *Introduction to Chemical Kinetics*. Academic Press, New York, 17 (1974).
  31. Still, W. C., N. G. J. Richards, W. C. Guida, M. Lipton, R. Liskamp, G. Chang, and T. Hendrickson. MacroModel, Version 2.5. Department of Chemistry, Columbia University, New York.
  32. Daniels, F. *Outlines of Physical Chemistry*. Wiley and Sons, London, 89-110 (1945).
  33. Galey, W. R., J. D. Owen, and A. K. Solomon. Temperature dependence of nonelectrolyte permeation across red cell membranes. *J. Gen. Physiol.* **61**:727-746 (1973).
  34. Diamond, J. M., and E. M. Wright. Biological membranes: the physical basis of ion and non-electrolyte selectivity. *Annu. Rev. Physiol.* **31**:581-646 (1969).
  35. Leo, A., C. Hansch, and D. Elkins. Partition coefficients and their uses. *Chem. Rev.* **71**:525-616 (1971).
  36. Fujita, T., J. Iwasa, and C. Hansch. A new substituent constant,  $\pi$ , derived from partition coefficients. *J. Am. Chem. Soc.* **86**:5175-5180 (1964).
  37. Painter, G. R., J. P. Shockcor, and C. W. Andrews. Application of molecular mechanics to the study of drug-membrane interactions, in *Advances in Molecular Modeling* (D. Liotta, ed.). JAI Press Inc., Greenwich, CT, 135-163 (1990).
  38. Gutknecht, J., and D. C. Tosteson. Diffusion of weak acids across lipid bilayer membranes: effects of chemical reactions in the unstirred layers. *Science (Washington D. C.)* **182**:1258-1260 (1973).

---

Send reprint requests to: Dr. George R. Painter, Division of Virology, Burroughs Wellcome Co., 3030 Cornwallis Road, Research Triangle Park, NC 27709.

---